Nuclear Magnetic Resonance Imaging of the Vitreous Body

Abstract. *Imaging with proton nuclear magnetic resonance is a valuable new tool for studying the vitreous body of the eye. It is particularly suited for the detection of vitreal liquefaction and intraocular hemorrhage because of the dependence of the signal on the physical environment of water. Conversely, the vitreous body provides a new model for studying changes in proton relaxation times of protein solutions in biological systems.*

Imaging with proton nuclear magnetic resonance (NMR) is a new method of clinical examination. Intrinsic differences in proton relaxation times among tissues allow excellent contrast in imaging normal structures and highly sensitive detection of pathological states. Significant biological application of NMR techniques is less than 15 years old (*1*). Most studies have centered on isolated intact tissue or whole cells, particularly cancer cells (*2*). These are complicated biological systems, and the conflicting interpretations of the results have reflected this complexity (*3*). Even with simple protein solutions there are numerous opinions as to the reason for altered relaxation mechanisms (*4*). The vitreous body of the eye provides a new model in which changes in the relaxation time of water protons, and therefore changes in image brightness, are due to the phase change from a gel to a liquid that accompanies collagen degradation and not to changes in the concentrations of constituents. A clear distinction between normal and pathological states can thus be established.

The vitreous body, a transparent connective tissue occupying the major portion of the mammalian eye, is composed of water (98 percent) and hyaluronic acid polymers interspersed in a mesh of collagen fibrils (*5*). In the young human eye the vitreous body is normally a gel (*6*). However, it may change to a liquid during normal aging and in a number of pathological processes, including retinitis pigmentosa, myopia, retinal tears, trauma, connective tissue disorders, and diabetes (*7*). Associated changes that may lead to blindness include hemorrhage into the posterior portion of the eye and retinal detachment (*8*). It has been difficult to assess the contributions of the vitreous body to such conditions because of its transparence. The present study was undertaken to determine the ability of NMR imaging to detect pathological changes in the vitreous body.

To simulate liquefaction, an enucleated bovine eye was injected with 0.2 cm^3 of a solution of collagenase (400 U/cm^3) prepared in Mg^{2+}- and Ca^{2+}-free phosphate-buffered saline and incubated at room temperature. The eye was examined by NMR imaging immediately after the injection and 12 hours later. To simulate intraocular hemorrhage, a second eye was injected posterior to the lens with 0.2 cm^3 of fresh human blood and imaged immediately, and a third eye was similarly injected and imaged after 12 hours. The NMR images were obtained with a small-bore (8-cm) superconducting magnet operating at a magnetic field strength of 1.44 T, corresponding to a proton resonance frequency of 61.4 MHz. The selective excitation technique was used for plane selection, and a partial saturation pulse sequence with spin-echo data acquisition (30-msec delay) was employed. The 90° to 90° interpulse delay ranged from 300 msec to 8 seconds, corresponding to imaging times of 0.8 to 15 minutes. Slice thickness was 3 mm with approximately 0.5 mm in-plane spatial resolution.

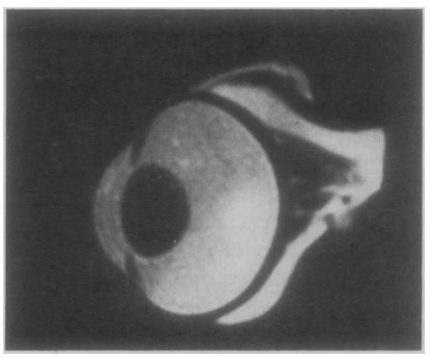

Fig. 1. Progressive saturation (1200/30 msec) image of a bovine eye 12 hours after injection with 0.2 cm^3 of a solution of collagenase (400 U/cm^3). Note the bright area at the posterior pole. This area of enhanced relaxation (shorter T_1) was absent immediately after injection. The anterior chamber, iris, lens, vitreous body, orbital fat, and muscle are clearly differentiated. The optic nerve is out of the image plane.

The images obtained at a pulse interval of 1.2 seconds are shown in Figs. 1 and 2. The images provide a detailed view of various ocular tissues, including the lens, sclera, iris, fat, muscle, optic nerve, and vitreous body. Contrasts in the vitreous body were not apparent at a 90° to 90° interpulse delay of 300 msec. Maximum visual contrast was observed at the 1200-msec delay time shown.

The basic difference between vitreous gel and vitreous liquid is that the latter does not have collagen fibrils (*9*). Treating vitreous gel with collagenase produces a liquid rheologically similar to that found in the vitreous body in various pathological states (*10*). The liquefied portion of the vitreous body in Fig. 1 appears brighter than the surrounding normal gel. The calculated proton longitudinal relaxation time (T_1) (*11*) of water in vitreous liquid (1590 msec) was markedly shorter than that of water in vitreous gel (1820 msec). Control eyes injected with normal saline and collagenase-treated eyes scanned immediately showed no variations in signal across the vitreous body. Thus the changes seen in Fig. 1—from a normal to a pathological state in the vitreous body—were due to the liquefaction produced by collagenase activity rather than a change in water content.

In the eyes injected with blood (Fig. 2) the limits of infiltration were clearly delineated. The increased signal intensity of the old blood implies a shortening of T_1. The reason for this enhancement of longitudinal relaxation is almost certainly related to clotting. Unlike other methods of imaging or examining the eye, areas posterior to the blood could still be

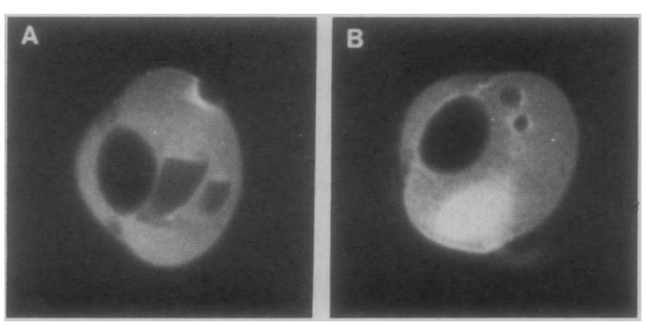

Fig. 2. (A) Eye injected with human blood and imaged within a few minutes. Two pockets of blood are seen as dark areas (the largest directly behind the lens), indicating that T_1 is longer for fresh blood than for the vitreous body. The point of entry of the needle can be seen at the sclera toward the top of the picture. (B) Eye injected with human blood and imaged after 12 hours. The T_1 is now much shorter than that of the vitreous body, suggesting a conformational change in proteins. There is no signal from the small air bubbles at the top of the picture because of the absence of protons. The optic nerve can be seen posterior to the hemorrhage.

examined without interference from the intraocular hemorrhage.

In conclusion, vitreous liquefaction and intraocular hemorrhage may be accurately assessed by proton NMR imaging. This approach may have important clinical applications, particularly in evaluating proliferative diabetic retinopathy, the most common cause of blindness in the United States for people under the age of 60 (*12*). Early detection of liquefaction and detailed studies of sequelae, including hemorrhage, appear feasible. Similar studies of the natural history of other ocular diseases may also be possible.

R. GILBERTO GONZÁLEZ
HONG-MING CHENG*
PATRICK BARNETT
Howe Laboratory of Ophthalmology, Harvard Medical School, and *Massachusetts Eye and Ear Infirmary, Boston 02114*

JAMES AGUAYO
BERT GLASER
Wilmer Ophthalmological Institute, Johns Hopkins Medical School, Baltimore, Maryland 21205

BRUCE ROSEN
C. TYLER BURT
THOMAS BRADY
Department of Radiology, Harvard Medical School, and *Massachusetts General Hospital, Boston 02114*

References and Notes

1. C. B. Bratton, A. L. Hopkins, J. W. Weinberg, *Science* **147**, 738 (1965); C. F. Hazelwood, B. L. Nichols, N. F. Chamberlain, *Nature (London)* **222**, 747 (1969b); R. Cooke and R. Wien, *Biophys. J.* **11**, 1002 (1971); P. C. Lauterbur, *Nature (London)* **242**, 190 (1973).
2. R. Damadian, *Science* **171**, 1151 (1971); D. P. Hollis, L. A. Saryan, H. P. Morris, *Johns Hopkins Med. J.* **131**, 441 (1972); W. R. Inch, J. A. McCredie, R. R. Knispel, R. T. Thompson, M. Pintar, *J. Natl. Cancer Inst.* **52**, 353 (1974).
3. R. Mathur-de Vre, *Prog. Biophys. Mol. Biol.* **35**, 103 (1979).
4. R. G. Bryant, *Annu. Rev. Phys. Chem.* **29**, 167 (1978); B. D. Sykes, W. E. Hull, G. H. Snyder, *Biophys. J.* **21**, 137 (1978).
5. E. Balazs, in *The Structure of the Eye*, G. K. Smelser, Ed. (Academic Press, New York, 1961), p. 293.
6. ———, in *New and Controversial Aspects of Retinal Detachment*, A. McPhersen, Ed. (Harper & Row, New York, 1968), p. 3.
7. F. I. Toletino *et al.*, *Vitreoretinal Disorders: Diagnosis and Management* (Saunders, Philadelphia, 1976), pp. 131, 144, 269–289, 379, 437.
8. C. C. Teng and H. H. Chi, *Am. J. Ophthalmol.* **44**, 335 (1957); G. W. Cibis, R. C. Watzke, J. Chua, *ibid.* **80**, 1043 (1975); M. Favre and H. Goldmann, *Ophthalmologica* **132**, 87 (1956).
9. E. Balazs, in *Biomedical Foundations of Ophthalmology*, T. D. Duane and E. A. Jaeger, Eds. (Harper & Row, Philadelphia, 1982), p. 2.
10. J. Aguayo, J. B. Miceli, B. M. Glaser, *Invest. Ophthalmol. Visual Sci.* **24** (No. 3), 158 (1983).
11. B. R. Rosen, I. L. Pykett, T. J. Brady, *J. Comput. Assisted Tomogr.*, in press.
12. R. Y. Foos, A. E. Kreiger, A. B. Forsyth, K. A. Zakka, *Ophthalmology* **87**, 122 (1980); M. D. Davis, *Arch. Ophthalmol.* **74**, 741 (1965).
13. Supported in part by NIH grant 1R01-EY04424 (to H.-M.C.) and in part by Technicare Corporation. T.B. is supported in part by National Cancer Institute research career development award 1-K04-CA00848-02.
* To whom requests for reprints should be sent.

22 August 1983; accepted 7 December 1983

Plasmodium falciparum Maturation Abolishes Physiologic Red Cell Deformability

Abstract. *Normal red cells deform markedly as they pass through the spleen and the peripheral capillaries. In these studies, the effects of* Plasmodium falciparum *infection and maturation on the deformability of parasitized red cells exposed to fluid shear stress in vitro were examined by means of a rheoscope. Red cells containing the early (ring) erythrocytic stage of the parasite have impaired deformability at physiologic shear stresses, and recover their normal shape more slowly. Red cells containing more mature parasites (trophozoites or schizonts) exhibit no deformation under the same conditions. These results provide a mechanism to explain the ability of the spleen to remove parasitized red cells from the circulation of both immune and nonimmune hosts.*

The ability of the normal red cell to deform like a liquid droplet when subjected to shear stress in vitro is well documented (*1*). The normal red cell (disk diameter 7 to 8 μm) also deforms markedly in vivo in order to pass through the interendothelial slits and basement membrane fenestrations of the spleen (*2*) and through peripheral capillaries with luminal diameters of 3 to 4 μm. The rotation of the red cell membrane around its cytoplasmic contents in a motion suggestive of a tank tread is particularly significant (*3*), and recent reports have shown that tank-treading occurs in capillaries both in vitro (*4*) and in vivo (*5*). This tank-treading motion reduces the hydraulic resistance to red cell passage through the capillary (*6*), and may also facilitate oxygen exchange between the red cell and the capillary endothelium. This report identifies a disease state (*Plasmodium falciparum* infection) characterized by a loss of red cell deformability and tank-treading in which the loss of red cell deformability presumably facilitates the splenic removal of parasitized red cells from the circulation.

Miller and his colleagues suggested previously that parasitized red cells are less deformable than normal red cells (*7*). However, at the time those studies were performed a technique for the continuous culture of malaria parasites in vitro (*8*) was not available; the investigators used mixtures of parasitized and unparasitized cells to perform measurements of macroscopic viscosity and resistance to passage through a filter. In these studies, we used the rheoscope (*1*) to define the effects of graded levels of shear stress on the deformability of *P. falciparum*–infected red cells. This was accomplished by measuring the elongation (length to width ratio) of infected and control (uninfected) red cells in the same microscopic fields, by determining the prevalence of tank-treading among infected and control cells in the same fields, and by measuring the time course of the recovery of cell shape after the abrupt release of the shear stress.

Plasmodium falciparum parasites were cultured in an environment with 3 percent oxygen and 3 percent carbon dioxide (*9*) according to the system devised by Trager and Jensen (*8*). Most studies were performed with the chloroquine-resistant Indochina I/CDC strain, although several experiments were also performed with the chloroquine-susceptible Honduras I/CDC strain (*10*). A knobless clone of the FCR-3 strain from The Gambia (clone D-4) (*10, 11*) was used to determine whether the observed changes in the deformability of parasitized red cells were associated with knob formation (*12*).

To produce parasitemias 15 percent or more for examination in the rheoscope without exhausting the ability of the culture medium to support parasite growth, we maintained heavily parasitized red cell suspensions at hematocrits near 1 percent and provided them with fresh medium two to three times daily. Red cells with trophozoites or schizonts from

Table 1. Red cell recovery time and *P. falciparum* infection. The characteristic shape-recovery time (t_c) is defined by a simple exponential fit of the time course of the recovery of cell length immediately after the release of a shear stress of 20 dyne/cm^2 (*17, 18*) as described by the equation:

$$\frac{L - L_f}{L_i - L_f} = e^{-t/t_c}$$

where L, L_i, and L_f are the instantaneous, initial, and final cell lengths, respectively, and t is the time after release of the shear stress. According to this formula, the elongation of a cell ($L - L_f$) is 36.8 percent of its initial value ($L_i - L_f$) at time t_c. The recovery times observed for red cells with rings were significantly longer than those of normal (uninfected) red cells ($t = 2.896$, $P < 0.005$).

Red cell type	t_c (seconds)	
	Mean	Standard deviation
Normal red cells	0.121*	0.029
Red cells with rings	0.137*	0.036

*$N = 70$.